

# An Implantable, Miniaturized SU-8 Optical Probe for Optogenetics-Based Deep Brain Stimulation

Bin Fan-*IEEE Student Member*, Ki Yong Kwon, -*IEEE Student Member*, Arthur J. Weber and Wen Li, *IEEE Member*

**Abstract**—This paper reports a method of making optical probes for optogenetics-based deep brain optical stimulation using SU-8, which effectively increases light coupling efficiency, has excellent mechanical stiffness, and reduces fabrication complexity. By mounting microscale LEDs ( $\mu$ LEDs) at the tip of a SU-8 probe and directly inserting the light source into deep brain regions, attenuation caused by light transmission in wave-guided structures such as optical fibers or optrodes can be minimized. Compared to silicon neural probes, SU-8 is more biocompatible and flexible, which can reduce brain damage. Parylene-C encapsulation can potentially improve the long-term biocompatibility and reliability of the device for chronic implantation. The functionality has been proven by clearly light-induced neural activity.

## I. INTRODUCTION

Brain-machine interfaces which achieve a connection between the brain and external devices have many medical applications on restoring motor control, such as patients suffering from spinal cord injury and stroke, and treating neurological disorders, such as patients with Parkinson's disease and depression [1][2]. Recently, optogenetics has drawn a lot of attention because it provides an effective way of manipulating a specific cell type by light stimulating microbial opsin expressed cells on a timescale of milliseconds [3]. Typically, light delivery into targeting areas is achieved using optical fibers or waveguides coupled to external laser diodes or microscale light emitting diodes ( $\mu$ LEDs). However, those laser diodes require high electrical power, which is an obstacle to achieve wireless operation of implanted device. In addition, it will be difficult to make a laser diode work at the maximum activation wavelength. On the other hand, using optical fibers or waveguides to guide light into targeting cells suffers from low coupling efficiency.

To tackle these drawbacks, in this paper, we present an approach by mounting  $\mu$ LEDs at the tip of a SU-8 probe and directly inserting the light source into deep brain regions. SU-8 negative photoresist has been used in a lot of biomedical applications. *In vitro* and *in vivo* testing have proven its biocompatible characteristics by cell viability and minimal

hemolytic activity [4]. Compared to silicon neural probes, SU-8 has a smaller Young's modulus [5][6], which makes it more flexible and thus causes less damage to the brain tissue.

## II. OPTICAL PROBE DESIGN AND FABRICATION

### A. Design of Optical Probe

In our design, we used SU-8 2000 negative photoresist, which is an improved formulation of SU-8. It can achieve over 200  $\mu$ m thick coating with a single spinning process. Besides, it is capable of making high aspect ratio structure and has very high optical transmission over 360 nm, which makes SU-8 2000 a perfect candidate for our design purpose [6].

As shown in the concept diagram (Figure 1), two layers of SU-8 photoresist were used in the fabrication, in which the top layer was 10% wider than the bottom one to encapsulate  $\mu$ LED chip. Several SU-8 anchors along the central line of the shank were designed to improve the bonding strength between the two SU-8 layers. The  $\mu$ LED chip end of the SU-8 shank is 10% smaller than the contact end to make it easier for penetrating into the brain. The overall device is encapsulated with Parylene coating to further protect the device from exposure to body fluid. The Parylene package also reduces the risk of wiring being broken due to the dangling and stretching during device implantation. The dimensions of the probe and the  $\mu$ LED chip are listed in Table 1.

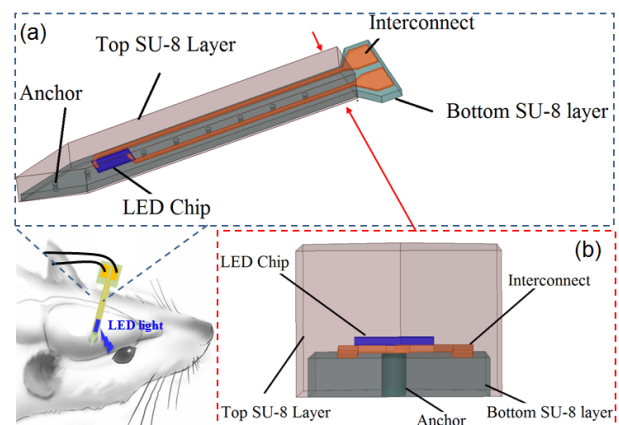


Figure 1: Conceptual diagram of the optical probe: (a) an overall view (b) a cross-section view.

Research supported by NSF CAREER ECCS-1055269.

Bin Fan, Ki Yong Kwon and Wen Li are with the Department of Electrical and Computer Engineering, East Lansing, MI, 48824, USA (phone: 517-355-3299; e-mail: fanbin@msu.edu).

Arthur J. Weber, is with Department of Physiology, Michigan state University, East Lansing, MI, 48824, USA

Table 1 Dimensions of the SU-8 probe and  $\mu$ LED (L: length, W: width, H: height)

Probe (L×W)	4.2mm×0.86mm
Top SU-8 layer (W×H)	0.49mm×0.28mm
Bottom SU-8 layer (W×H)	0.42mm×0.12mm
Anchor diameter	0.03mm
Anchor interval	0.4mm
$\mu$ LED (L×W×H)	0.550mm × 0.290mm × 0.100mm

### B. Fabrication process

A 3'' silicon carrier wafer was cleaned by isopropanol, acetone and deionized water. (a) 5 $\mu$ m Parylene C was deposited (PDS 2010, Specialty Coating System, Inc), followed by spinning the first layer of  $\sim$ 120  $\mu$ m SU-8 2075. (b) The first layer of SU-8 was patterned using standard lithography. (c) A 0.5  $\mu$ m layer of Cu was deposited on the first SU-8 layer using a thermal evaporator (Auto 306, Edward, Inc). (d) The Cu layer was patterned and wet etched to form connection between pads and leads. While copper was used in the prototype as a proof-of-concept, devices for chronic implantation will use noble metal such as gold and platinum. During the copper patterning step, because the optical probe stuck out of the wafer, thick photoresist residue was observed at the edge of the wafer after photolithography. As a result, short circuit was formed between the anode and cathode of  $\mu$ LED, as shown in Figure 2(b). This is solved by increasing photoresist spinning speed by 50% and reducing 20% exposure time, which can significantly reduce the residue without undercutting too much copper. (e) S1813 photoresist was spun on top of the copper leads and exposed contact areas with  $\mu$ LED chips. The surface was then treated with O<sub>2</sub> plasma (PX-250 plasma system, Nordson, Inc) with 500 mTorr base pressure and 100 W power to remove photoresist residue on top of the anode and cathode openings. Then low melting point (LMP) solder (melting point at  $\sim$ 62  $^{\circ}$ C, 144 ALLOY Field's Metal, Rotometals, Inc) was applied to the interconnects of the copper leads. (f) The wafer was immersed in acid solvent and suspended  $\mu$ LED chips (Samsung, Inc) were self-assembled onto the corresponding anode and cathode contacts. (g) S1813 was removed using acetone followed by IPA and DI water rinse. (h) A  $\sim$ 280  $\mu$ m layer of SU-8 was spun and patterned to form the probe shape with a slanted tip for easy penetration of rat's brain without removing the dura. A dual spin coating process was used in order to achieve a better uniformity of the SU-8 coating and prevent wrinkles appearing by thermal stress during the post baking of SU-8. This was done by spinning a first layer of  $\sim$ 120  $\mu$ m SU-8 and then another layer of  $\sim$ 160  $\mu$ m SU-8. (i) The LMP solder was applied on to pads in the solvent bath. Copper wires were bond to pads by melting LMP. Epoxy was applied to strengthen the bonding between pads and copper wires. Then SU-8 optical probes were released from the silicon wafer. (j) Finally, the whole device was encapsulated with  $\sim$ 10  $\mu$ m conformal Parylene C coating.

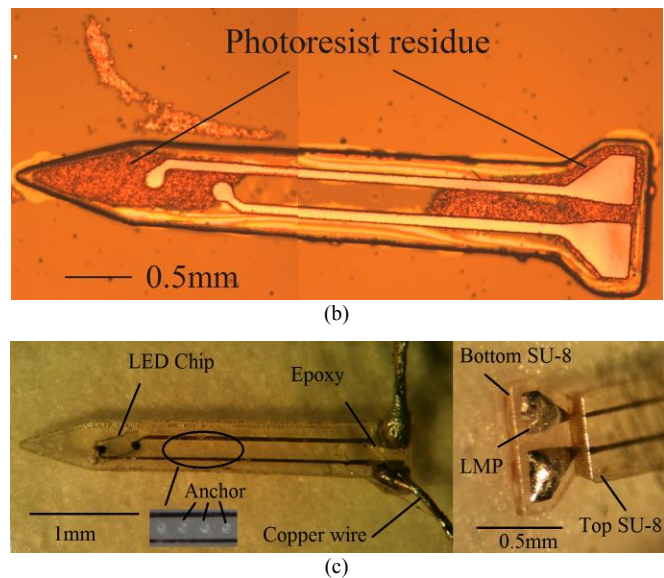
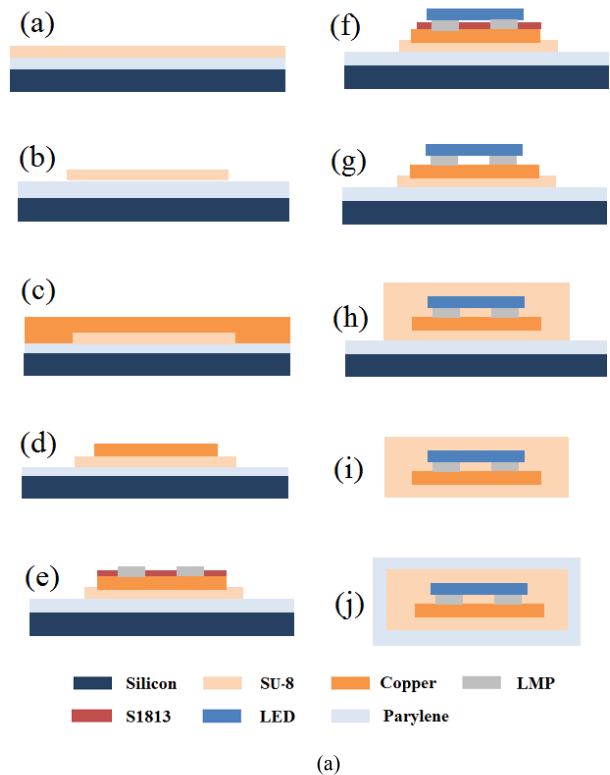


Figure 2 (a) The process flow for making the penetrating optical probe. (b) A optical probe with thick photoresist residue at the edge. (c) A fabricated optical probe with a  $\mu$ LED mounted on the tip

## III. EXPERIMENTAL RESULTS

### A. Electrical properties

The current-voltage curve of the  $\mu$ LED was characterized using a 4145B semiconductor parameter analyzer, (Hewlett Packard, Inc), as plotted in Figure 3 (a). The forward threshold of this  $\mu$ LED is around 2.6V. The typical voltages applied to  $\mu$ LED and their corresponding input powers are listed in Table 2.

Table 2 Typical parameters using for optical stimulation

Applied voltage	Input current	Power consumption
3.0 V	11.2mA	33.6mW
3.2 V	22.6mA	72.4mW
3.4 V	38.2mA	130mW

### B. Optical properties

The spectrum of light intensity coming through a  $\sim 280 \mu\text{m}$  thick top layer of SU-8 is shown in Figure 3 (b). The peak intensity was located between 450 nm and 460 nm, which is within the maximum activation wavelength region [7].

To study the light attenuation due to the SU-8 coating, we measured the outcoupling light intensities of probes with a  $280 \mu\text{m}$  SU-8 layer coating and without SU-8 coating, respectively. The data was recorded from a digital power meter (Model 815 Series, Newport, Inc) through a RHA 2000 evaluation board (Intan Technologies, Inc). As plotted in Figure 3 (c), the light intensities of the probes with the SU-8 coating are 23 % and 7.1 % higher than those without SU-8, when the applied voltages are 3.2 V and 3.4 V, respectively. This could be mainly attributed to the curvature of the top SU-8 layer formed due to the thermally-induced polymer reflow, which effectively collimates the light of the embedded  $\mu\text{LED}$  chip. The SEM image, (HitachiS-4700, Hitachi, Inc) and profilometry, (NanoMap-500LS, Nanomap, Inc) of the probe surface were taken as shown in Figure 3(d) where clear curvature is shown. However, it is also observed that, when the applied voltage increased to 3.6 V, the intensity of SU-8 coated probe was slightly lower (7.6 %) than that of uncoated probe. This inconsistency may be due to the overheating effect of the  $\mu\text{LED}$  at a high input voltage, which deteriorates SU-8 and results in the reduced optical transparency. Besides, the high noise level of measurement instrument might contribute to this as well. The variance of the data recorded from evaluation board is quite noisy as shown from the error bars.

The scattering property of  $\mu\text{LED}$  light was studied in gelatin where the  $\mu\text{LED}$  was driven with 2.74 V input voltage and 7 mW total power consumption as shown in Figure 3(e). The light propagation profile was plotted in Matlab (Figure 3b) where blue spectra (450 ~ 495 nm) were extracted. The 90 % of the light intensity was within an elliptical-shaped scattering boundary ( $\sim 10 \text{ mm}$  in width and  $\sim 5 \text{ mm}$  in length), which enables optical excitation of a large population of neurons. Our previous study showed that 7 mW power consumption of a  $\mu\text{LED}$  resulted in a local temperature increase of  $\leq 0.5^\circ\text{C}$ , which is a conservative limit on the temporarily allowable temperature rise in brain tissue adjacent to the implants [8].

### C. In-vivo LFP signal recordings

*In vivo* local field potential (LFP) upon optical stimulation was recorded in the unilateral visual cortex of an anesthetized, channelrhodopsin-2 (ChR2) expressed rat as shown in Figure 4 (a). The rat was anesthetized with a mixture of ketamine and xylazine according to its weight. After the rat was fully

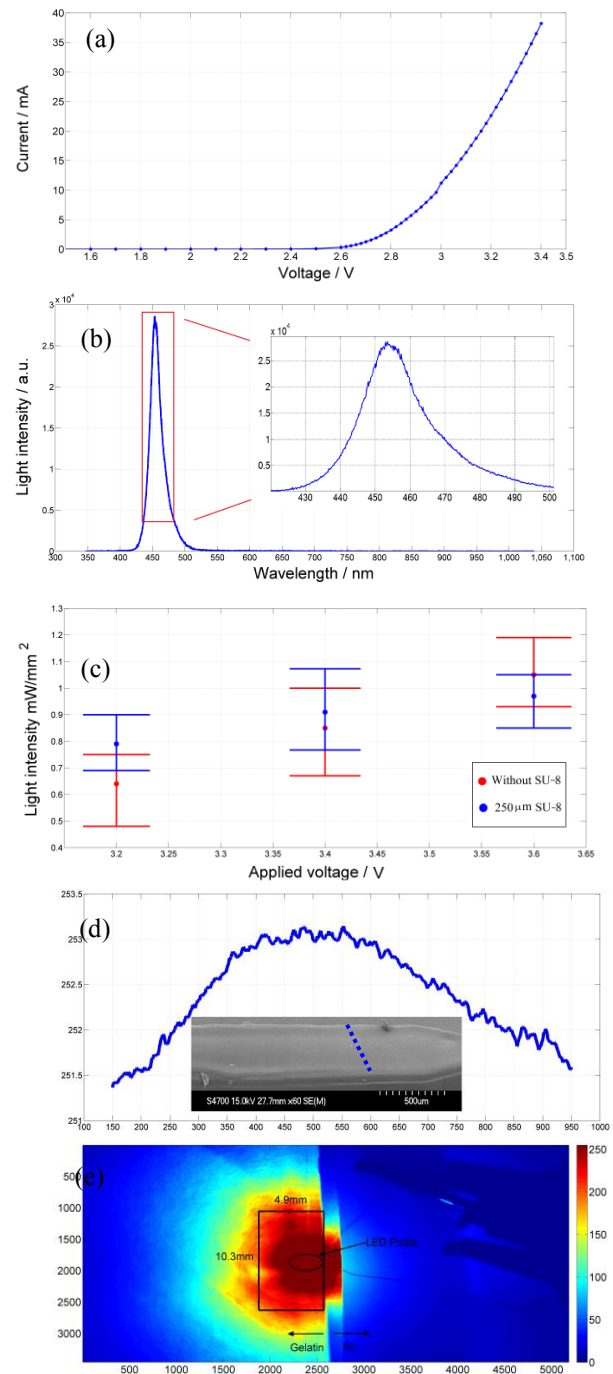


Figure 3 Electrical and optical characteristics of SU-8 probe. (a)  $I$ - $V$  curve of  $\mu\text{LED}$ . (b) Spectrum of light emitting from  $\mu\text{LED}$  chip with a  $\sim 280 \mu\text{m}$  SU-8 coating. (c) A comparison of light intensity of optical probe coated with and without SU-8. (d) SEM image and profilometry of the SU-8 probe (e) Light scattering property measured in gelatin.

down, it was placed on a towel with heating pads underneath, which prevents the rat from losing too much its body temperature during the surgery. Then the head of rat was stabilized in a stereotaxic apparatus through ear bars. After shaving hairs, 70 % alcohol and betadine were used to clean and disinfect the skin of the skull three times in turn. Then a rostral-caudal incision was made to expose the bony skull.

Drilling was used to remove skullcap to prevent bleeding and minimize the damage to the cortical area. A tungsten probe was used to record LFP that was connected to a pneumatic pump to precisely control the penetration depth. The light-evoked signal was amplified and recorded using an RHA2000 amplifier and evaluation board (Intan Technologies). Significant changes in neural activity were recorded when the  $\mu$ LED was driven by  $3.2 V_{\text{peak}}$  pulses with a 100 ms pulse width. Specifically a  $3.2 V_{\text{peak}}$  input voltage resulted in the light intensity of  $\sim 0.8 \text{ mW/mm}^2$ , which was sufficient for optical excitation of ChR2 expressed neurons, as demonstrated in *in vivo* testing. A clear light-induced neural activity was observed in time-domain LFP (1~100Hz) as shown in Figure 4(b), which demonstrates the efficacy of deep brain stimulation using the fabricated SU-8 optical probe. As comparison, LFP oscillations excited with  $3.0 V_{\text{peak}}$  and  $3.4 V_{\text{peak}}$  pulses were recorded. The results show that the average amplitude of LFP oscillations increased from  $400 \mu\text{V}$  to  $750 \mu\text{V}$  when the input voltage of LED was changed from  $3.0 V_{\text{peak}}$  to  $3.4 V_{\text{peak}}$ . This is mainly due to the increased light intensity, which can activate more neurons in a larger range.

#### IV. CONCLUSION

This paper reports a method of making optical probes for optogenetics-based deep brain optical stimulation using SU-8. The electrical and optical analyses show that the SU-8 layer not only remains the central irradiation wavelength of the  $\mu$ LED but also effectively enhance the light outcoupling intensity, which establish a basis of using SU-8 photoresist as a probe material for optogenetics. An accelerating soaking test is ongoing. Although in this paper we only present the preliminary prototype of a single-shank probe with the functionality of stimulation, our current work focuses on the integration of microelectrodes with the SU-8 optical probe to achieve simultaneous recording and stimulation. The success of our previous research work also demonstrates the potential of fabricating multi-shank probes for high-density optogenetic stimulation and recording [9][10].

#### REFERENCES

- [1] M. A. Lebedev and M. A. L. Nicolelis, "Brain-machine interfaces: past, present and future," *Trends Neurosci.*, vol. 29, no. 9, pp. 536–546, Sep. 2006.
- [2] K. Y. Kwon, B. Sirowatka, W. Li, and A. Weber, "Opto- $\mu$ ECoG array: Transparent  $\mu$ ECoG electrode array and integrated LEDs for optogenetics," in *2012 IEEE Biomedical Circuits and Systems Conference (BioCAS)*, 2012, pp. 164–167.
- [3] A. M. Aravanis, L.-P. Wang, F. Zhang, L. A. Meltzer, M. Z. Mogri, M. B. Schneider, and K. Deisseroth, "An optical neural interface: in vivo control of rodent motor cortex with integrated fiberoptic and optogenetic technology," *J. Neural Eng.*, vol. 4, no. 3, pp. S143–156, Sep. 2007.
- [4] K. V. Nemani, K. L. Moodie, J. B. Brennick, A. Su, and B. Gimi, "In vitro and in vivo evaluation of SU-8 biocompatibility," *Mater. Sci. Eng. C*, vol. 33, no. 7, pp. 4453–4459, Oct. 2013.
- [5] E. J. Boyd and D. Uttamchandani, "Measurement of the Anisotropy of Young's Modulus in Single-Crystal Silicon," *J. Microelectromechanical Syst.*, vol. 21, no. 1, pp. 243–249, Feb. 2012.
- [6] SU-8 2000 Permanent Epoxy Negative Photoresist Datasheet.
- [7] F. Zhang, V. Gradinaru, A. R. Adamantidis, R. Durand, R. D. Airan, L. de Lecea, and K. Deisseroth, "Optogenetic interrogation of neural circuits: technology for probing mammalian brain structures," *Nat. Protoc.*, vol. 5, no. 3, pp. 439–456, Mar. 2010.
- [8] P. Andersen and E. I. Moser, "Brain temperature and hippocampal function," *Hippocampus*, vol. 5, no. 6, pp. 491–498, 1995.
- [9] K. Y. Kwon, A. Khomenko, M. Haq, and W. Li, "Integrated slanted microneedle-LED array for optogenetics," in *2013 35th Annual International Conference of the IEEE Engineering in Medicine and Biology Society (EMBC)*, 2013, pp. 249–252.
- [10] K. Y. Kwon, B. Sirowatka, A. Weber, and W. Li, "Opto- $\mu$ ECoG array: a hybrid neural interface with transparent  $\mu$ ECoG electrode array and integrated LEDs for optogenetics," *IEEE Trans. Biomed. Circuits Syst.*, vol. 7, no. 5, pp. 593–600, Oct. 2013.

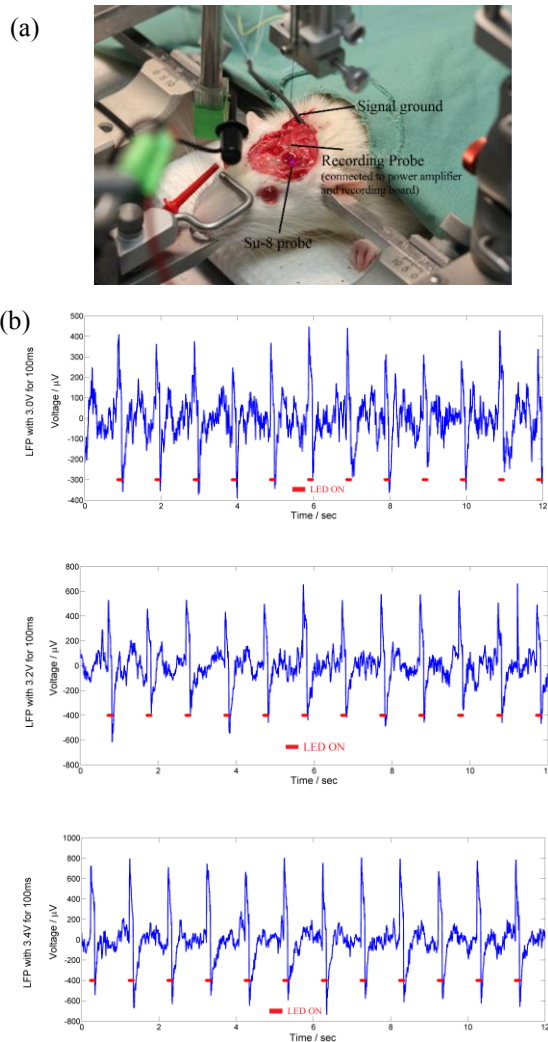


Figure 4: Demonstration of the efficacy of the deep brain optical stimulation using the fabricated probe in the rat's brain: (a) the experiment setup and (b) the recorded LFP with the  $\mu$ LED input voltage of 3.0V, 3.2 V and 3.4V.